



HAL
open science

Chaotic filtering of moving atoms in pulsed optical lattices by control of dynamical localization

Thibaut Jonckheere, M.R. Isherwood, T.S. Monteiro

► **To cite this version:**

Thibaut Jonckheere, M.R. Isherwood, T.S. Monteiro. Chaotic filtering of moving atoms in pulsed optical lattices by control of dynamical localization. *Physical Review Letters*, 2003, 91 (25), pp.253003. 10.1103/PhysRevLett.91.253003 . hal-00005679

HAL Id: hal-00005679

<https://hal.science/hal-00005679>

Submitted on 31 May 2023

HAL is a multi-disciplinary open access archive for the deposit and dissemination of scientific research documents, whether they are published or not. The documents may come from teaching and research institutions in France or abroad, or from public or private research centers.

L'archive ouverte pluridisciplinaire **HAL**, est destinée au dépôt et à la diffusion de documents scientifiques de niveau recherche, publiés ou non, émanant des établissements d'enseignement et de recherche français ou étrangers, des laboratoires publics ou privés.

Chaotic Filtering of Moving Atoms in Pulsed Optical Lattices by Control of Dynamical Localization

T. Jonckheere,* M. R. Isherwood, and T. S. Monteiro

Department of Physics and Astronomy, University College London, Gower Street, London WC1E 6BT, United Kingdom

(Received 17 April 2003; published 18 December 2003)

We propose a mechanism for a velocity-selective device which would allow packets of cold atoms traveling in one direction through a pulsed optical lattice to pass undisturbed, while dispersing atoms traveling in the opposite direction. The mechanism is generic and straightforward: for a simple quantum kicked rotor pulsed with unequal periods, the quantum suppression of momentum diffusion (dynamical localization) yields momentum localization lengths L which are no longer isotropic, as in the standard case, but vary smoothly and controllably with initial momentum.

DOI: 10.1103/PhysRevLett.91.253003

PACS numbers: 32.80.Pj, 05.45.Mt, 05.60.-k

There is much current interest in the development of new techniques to manipulate cold atoms. Recent work in atom optics has resulted in new devices termed “atom chips” [1,2] where cold atoms may be trapped and guided by fields above a solid substrate. Within such an atom chip, techniques to split, transport, and otherwise control the traffic of atoms can play an important role.

In addition, cold atoms in pulsed or driven optical lattices have become a paradigm in the field of quantum chaos: experiments on sodium and cesium atoms [3] provided a textbook demonstration of dynamical localization (DL) [4,5], the quantum suppression of classical chaotic diffusion. The corresponding classical motion is fully chaotic for sufficiently strong driving. The energy of the system grows diffusively with each consecutive pulse or “kick”: in the absence of phase-space barriers, which are present only in the regular regime, the average energy $\langle p^2 \rangle$ of the particles is unbounded and this diffusive increase in energy continues indefinitely. It is characterized by a diffusion rate D_0 , i.e., $\langle p^2 \rangle = D_0 t$. However, in the *quantum* case this process is suppressed on the time scale of the so-called “break time” $t^* \sim D_0/\hbar^2$ [6].

The series of ground-breaking experiments in [3] was followed by other experiments with optical lattices probing a wide range of quantum chaos phenomena including dynamical tunneling [7], the effect of quantum loss of coherence on dynamical localization [8], and quantum accelerator modes [9].

Here we show that a straightforward modification of the quantum chaos experiments can form the basis for a device to control the traffic of cold atoms moving along a channel in, say, an atom chip by selecting a specified velocity. In these experiments the atoms experience a periodically pulsed or driven standing wave of light. By pulsing the usual sinusoidal lattice with slightly different periods we show that the diffusion rate is not only momentum dependent, i.e., $D = D(p)$, but takes a particular smooth and controllable form. We investigated the quantum dynamics and found that they are associated with a corresponding local break time $t^*(p) \sim D(p)/\hbar^2$. Since

these break times vary by ~ 2 orders of magnitude, this represents a strong effect. By simply varying the pulsing periods, we can specify a value of p , so that for particles moving in one direction $D^+(p) \sim 0$, which means they absorb little energy, while particles moving in the opposite direction experience an enhanced diffusion rate $D^-(-p) > D_0$. While in the classical case, this effect is confined to a very narrow parameter range and small t , we show here that for the equivalent quantum system, this “filtering effect” is, in fact, controlled by the dynamical localization and remains effective over a wide and experimentally accessible parameter range. The ratio of energy absorbed by particles moving in opposite directions classically is $\sim D^+(p)/D^-(p)$ for short times and ~ 1 for longer t ; in the quantum case, due to dynamical localization, the corresponding ratio is $[D^+(p)/D^-(p)]^2 \sim \text{const}$ for all $t > t^*$. We stress that selecting the required filter parameters involves no knowledge of the details of the underlying classical trajectories so is a quite generic procedure. While the study of this novel regime of controllable localization in a modified standard map is quite general, we focus on the most favorable parameters for a cold-atom experiment since this represents a real application of a fundamental physics phenomenon.

In the dynamical localization experiment of [3,7,8], the dynamics is approximately given by the delta-kicked rotor Hamiltonian: $H = \frac{p^2}{2} - K \cos x \sum_n \delta(t - nT)$ where K is the kick strength. The classical dynamics is obtained by iterating the well-known “standard map”: $x_{i+1} = x_i + p_i T$; $p_{i+1} = p_i + K \sin x_{i+1}$. In the standard map, we can take $T = 1$, without loss of generality, but for the proposed system we use a repeating cycle of unequally spaced kicks. For simplicity, we take a length-2 cycle, with the spacing between kicks alternating between T_1 and T_2 . The Hamiltonian is now given by

$$H = \frac{p^2}{2} + V(x) \sum_{n=0}^{\infty} \sum_{M=1}^2 \delta\left(t - nT_{\text{tot}} + \sum_{i=1}^M T_i\right) \quad (1)$$

with $T_{\text{tot}} = T_1 + T_2$. This means that the first kick after $t = 0$ is at $t = T_1$, the second kick at $t = T_1 + T_2$, the next one at $t = T_1 + (T_1 + T_2)$, and so on. We will consider only a small deviation from equally spaced kicks, which can be defined with the small parameter b , $T_1 = 1 + b$, $T_2 = 1 - b$. If required, the spatial symmetry can be broken by adding to the sine potential a linear term which alternates in sign: $V(x) = -[K \cos x + Ax(-1)^j]$, where j is the kick number. This Hamiltonian leads to the map,

$$\begin{aligned} x_i &= x_{i-1} + p_{i-1}(1 + b), \\ p_i &= p_{i-1} + K \sin x_i + A, \\ x_{i+1} &= x_i + p_i(1 - b), \\ p_{i+1} &= p_i + K \sin x_{i+1} - A. \end{aligned}$$

This classical map was investigated previously [10] in the regular regime, where the diffusion in p is bounded by regular tori, for rational b there is a long-ranged periodicity in the dynamics, and pairs of tori are distributed asymmetrically around $\langle p \rangle = 0$, leading to classical distributions with $\langle p \rangle \neq 0$ and resulting in a type of mixed-phase space ratchet. Here we investigate this map in the chaotic regime for unbounded diffusion: in the expressions below, whether b is rational or not is immaterial. We have also investigated the equivalent quantum behavior. Since the Hamiltonian involves only delta kicks, we consider the usual time evolution operator in a matrix representation using a plane-wave basis. We find that while single kicks couple different quasimomenta, the combined time evolution operator for two kicks does not. Hence it is most convenient to iterate the two-kick time-evolution operator. In the usual plane-wave basis $|n\rangle = \frac{1}{2\pi} \exp(inx)$, this takes the form of a matrix $\hat{U}(2)$ with elements:

$$\begin{aligned} \langle n|U^q|l\rangle &= e^{-i[(1+b)(l+q)^2\hbar]} \sum_j e^{-i(1-b)(j+qa)^2\hbar} J_{l-j+ka}\left(\frac{K}{\hbar}\right) \\ &\times J_{j-n-ka}\left(\frac{K}{\hbar}\right), \end{aligned} \quad (2)$$

where q is a quasimomentum, $ka = \text{int}(q - A)$, and $qa = q - A - ka$. We solve for the quantum time evolution by simply iterating repeatedly $\psi(2) = \hat{U}\psi(t=0)$. In Fig. 1 we demonstrate the effect on two quantum wave packets by iterating Eq. (2) over 50 pairs of kicks for two different sets of parameters chosen to correspond to experimentally accessible values. We show that the device functions as a sort of Maxwell demon: while packets moving to the right pass the pulsed lattice relatively unperturbed, those moving to the left are strongly dispersed. Below we analyze this effect.

For the standard map, at the lowest level of approximation, the classical momenta at consecutive kicks are uncorrelated and evolve in time as a ‘‘random walk.’’ It is characterized by linear energy growth and a diffusion

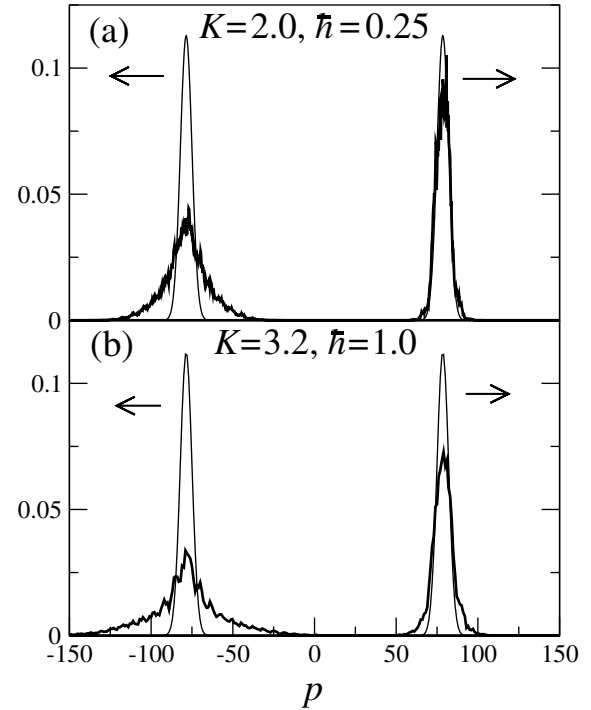


FIG. 1. Demonstration of the filtering effect: the figure compares the effect of 50 pairs of pulses on two quantum wave packets moving in opposite directions. Initial wave packets are shown with a thin line, while the final wave packets are shown with a bold line. Parameters: (a) for kick strength $K = 2.0$, $\hbar = 0.25$, and (b) for $K = 3.2$, $\hbar = 1.0$. The values of A and b are, in both cases, $\pi/2$ and 0.01 , respectively. The initial wave packets are centered around $\pm p_0$, with $4bp_0 = \pi$. The initial widths are similar to the standard experimental values. The figure shows that while the right-moving wave packet is only slightly perturbed, the left-moving one is strongly dispersed.

rate D_0 , i.e., $\langle p^2 \rangle = D_0 t$ where $D_0 = K^2/2$. However, correlations between sequences of consecutive kicks give important corrections to the diffusion coefficient. The two-kick correlation, for example, originates from correlations between adjacent kicks but one, $\langle V'(x_i)V'(x_{i-2}) \rangle$, and gives a correction $-K^2 J_2(K)$ to the diffusion coefficient. The diffusion coefficient, including the first corrections, is $D_0 = K^2[1/2 - J_2(K) - (J_1(K))^2 + \dots]$ [11,12]. These corrections have even been measured experimentally with cold cesium atoms in pulsed optical lattices [13].

For the Hamiltonian in Eq. (1), the correlations take a modified form. The corrections they induce are now momentum dependent: for an ensemble of particles with initial momentum p_0 , the average energy spread at time t is given by

$$\begin{aligned} \langle (p - p_0)^2 \rangle &= K^2 t \left\{ \frac{1}{2} - \frac{1}{2} [J_1(K(1+b))^2 + J_1(K(1-b))^2] \right. \\ &\quad \left. - K^2 \Phi(t) C(2, p_0) + \dots \right\}, \end{aligned} \quad (3)$$

where

$$C(2, p_0) = J_0(2bK) \cos[2p_0b - A(1 - b)] \\ \times [J_2(K(1 + b)) + J_2(K(1 - b))]$$

and

$$\Phi(t) = \frac{1 - J_0(2bK)^{t-2}}{1 - J_0(2bK)^2}.$$

Higher order correlations (four-kick, etc.) involve more Bessel functions, and induce corrections that may become significant over part of the parameter range, but Eq. (3) has the main features. The first correction in Eq. (3) is due to three-kick correlations, and is very similar to the $J_1(K)^2$ correction for the standard map. The $C(2, p)$ term is the modified version of the two-kick correlation term which for the standard map took the form $-K^2 J_2(K)$. This term has several important properties. First, it is p dependent with a single, simple $\cos[2pb - (1 - b)A]$ form. Particles with different momenta will absorb energy at different rates. Note that this is also the case for the $A = 0$ case: the role of linear potential is simply to specify the symmetry of this correction term, not its magnitude. Second, it has a non-trivial time dependence, given by the function $\Phi(t)$. We are interested in the regime of small b , where $bK \ll 1$ (see below). One has then $J_0(2bK) \simeq 1 - (bK)^2$. For $t \ll 1/(bK)^2$, $\Phi(t)$ has a linear behavior ($\sim t/2$), and the $C(2, p)$ term appears as a correction to the diffusion coefficient, as in the standard map. However, for larger t , $\Phi(t)$ saturates to the value $1/(2(bK)^2)$, and the two-kick correlation does not modify the energy growth anymore. We note that another system with momentum dependent diffusion has been investigated [14]: an asymmetric double-well lattice was found to yield asymmetric diffusion about $p = 0$. However, for that system, $D(p)$ has no particular symmetry over a larger scale in p and had complex oscillations with respect to p , from classical correlations yielding a many term Fourier series. Hence, they are not suitable for the velocity selector we propose here since one cannot control the form, the position, or the depth of the maxima and minima of $D(p)$. Here, we can simply by adjusting the small parameter b . We note that if b becomes large a one-kick correlation term can substantially modify the results.

All the expressions simplify considerably if we consider that $b \sim 0.01$ is a small deviation from period-one pulses, so $bA, bK \ll 1$. For times $t \ll 1/(bK)^2$, we can write

$$\langle (p - p_0)^2 \rangle = K^2 t \left[\frac{1}{2} - J_1(K)^2 - J_2(K) \cos(2p_0b - A) \right]. \quad (4)$$

Hence we have a local diffusion coefficient of the form $D(p) \simeq D_0 - C(2, p)$, where $D_0 \simeq K^2[1/2 - J_1(K)^2]$.

Figure 2 shows a comparison of this formula to numerical results: the average energy spread after 20 kicks is plotted as a function of K , for an ensemble of 400 000 particles with a narrow initial momentum distribution

around $p_0 = \pi/(4b)$, with $b = 0.005$ and $A = \pi/2$. For these values, one has $\cos(2p_0b - A) = 1$. For clarity, we have removed the p -independent contribution D_0 . We see that the numerical results agree very well with the formula (4), showing the $J_2(K)$ oscillations. For the larger values of K shown on the figure, the effect of the function $\Phi(t)$ begins to be noticeable, and formula (4) overestimates the result. The full analytic formula (3) is also shown, with an excellent agreement over the whole range of K .

Figures 3(a) and 3(b), shows the average energy spread as a function of the initial momentum p_0 , for two different sets of parameters. In each case both the classical and the quantum results are shown. For both quantal and classical diffusion, we obtain, as expected from Eq. (4), a cosine behavior in p_0 , with a period π/b . In 3(a), the number of kicks has been chosen to obtain the same maximum energy spreading for the quantum and the classical results; this shows clearly that the quantum minimum of the energy spreading is much lower than the classical one. Note that while the classical result is transient (the classical energy increases without bound) the quantum energy is at the asymptotic value.

We can now fully understand the results in Fig. 1: the “unperturbed” wave packets correspond to $p_0 = \pi/(4b)$, a minimum of the $\cos(2p_0b - A)$ function with $D \sim 0$ and $t^* \sim 1$. The dispersed wave packets correspond to the maximum at $p_0 = -\pi/(4b)$ where $D \sim K^2$ and here $t^* \sim 100$. We note that the effect is strong over a broad band of momenta around the minima and maxima at $p_0 = \pm\pi/(4b)$. The break time, which gives the time needed by the quantum system to localize, is proportional to the diffusion coefficient, so that near a maximum of the diffusion coefficient, the quantum system takes longer to localize. In contrast, near a minimum, the quantum system not only absorbs energy rather slowly, it also localizes more quickly and the quantum wave packet absorbs energy for a shorter time. Since $t^*(p_0) \sim D(p_0)/\hbar^2$, while the ratio of

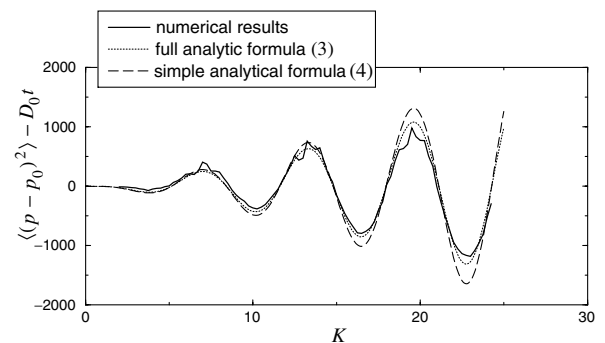


FIG. 2. Average energy spread as a function of K , for an ensemble of 400 000 particles with a narrow initial momentum distribution around $p_0 = \pi/(4b)$, with $b = 0.005$ and $A = \pi/2$. The $D_0 t$ term has been removed (see text). The numerical results are compared to the simple formula (4), valid for $t \ll 1/(bK)^2$, and to the full analytical formula (3).

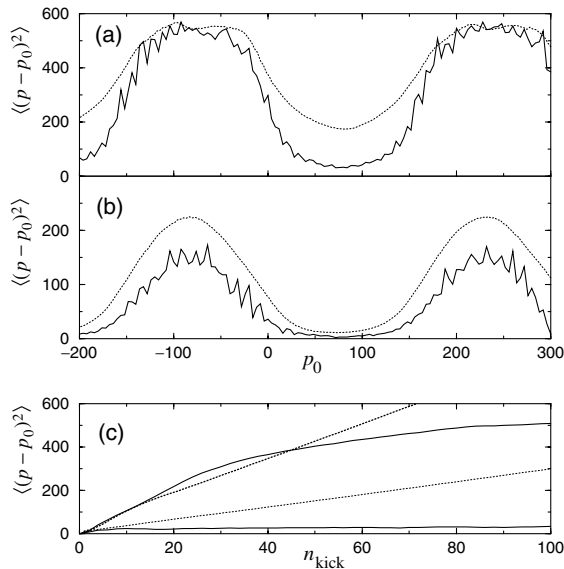


FIG. 3. (a),(b) Average energy spread as a function of initial momentum, in the classical case (dotted curve) and the quantum case (full curve). The parameters are the following: (a) $K = 3.2$, $\hbar = 1$, 60 kicks for the classical curve, 200 kicks for the quantum curve; (b) $K = 1.7$, $\hbar = 0.25$, 100 kicks for the classical curve, 100 kicks for the quantum curve. In both cases, $A = \pi/2$ and $b = 0.01$. In (a), the number of kicks in the classical case has been chosen to obtain the same maximum value for the energy spread as in the quantum case. The results show clearly that the diffusion coefficient oscillates as a function of p , with period π/b , and that the minimum of the diffusion coefficient is lowered in the quantum case compared to the classical one. (c) Average energy spread as a function of kick number, for two wave packets: one initially centered around $p_0 = \pi/(4b)$ (the two lower curves), the other initially centered around $p_0 = -\pi/(4b)$ (the two upper curves). The classical results are shown as dotted curves, while the quantum results are shown as full curves. One can see that the quantum wave packet with slow energy spread localizes extremely quickly, while the other wave packet takes a much longer time to localize. Parameters: $K = 3.2$, $b = 0.01$, $A = \pi/2$, and $\hbar = 1$ in the quantum case.

the maximum and minimum classical diffusion coefficient (or energy spread) is of the order of D_+/D_- , for the quantum system we obtain ratios for the energy spread of the order of $(D_+/D_-)^2$. In Fig. 3(a) ($K = 3.2$), for example, the ratio D_+/D_- is roughly of the order of 3, while the ratio of the quantum energy spreads is roughly 9. This enhancement due to dynamical localization is further illustrated in Fig. 3(c), where the energy of the two wave packets [one initially centered around $p_0 = \pi/(4b)$ (minimum), the other around $p_0 = -\pi/(4b)$ (maximum)] is plotted as a function of the kick number, for the classical and the quantum cases, for $K = 3.2$. One sees that the quantum wave packet with the slowest energy spread localizes very quickly (a few kicks are enough), while the other wave packet takes a much longer time to localize. We note that $A = 0$ produces similar results, with the exception that minima are shifted to

$p_0 = 0$ and integer multiples of π/b , while maxima occur at integer multiples of $\pi/(2b)$. Wave packets started between these points localize with asymmetric momentum distributions.

In summary, the filtering device results from a combination of two physical processes. The first process is a momentum-dependent diffusion coefficient of a particular simple form which enables one to select the velocities of interest by adjusting the magnitude of b . The second process is dynamical localization, which enhances the classical effect by localizing quickly (slowly) the quantum wave packet which absorbs energy slowly (fast).

T. M. thanks Thomas Dittrich, Sergej Flach, and Holger Schanz for helpful discussions. M. I. acknowledges the EPSRC for financial support. The work was supported by EPSRC Grant No. GR/N19519.

Note added.—Since submission of this Letter, a proof-of-principle version of the system we proposed here has been implemented experimentally by Jones *et al.* [15] for $A = 0$ and $b \simeq 0.1$ but otherwise with the parameters of our Figs. 1 and 3. An effective filter would, however, require smaller values of $b \simeq 0.01$ which have not yet been attempted.

*Present address: Centre de Physique Theorique, Campus de Luminy, Case 907, 13288 Marseille Cedex 9, France.

- [1] E. A. Hinds, C. J. Vale, and M. G. Boshier, *Phys. Rev. Lett.* **86**, 1462 (2001).
- [2] W. Hänsel, P. Hommelhoff, T.W. Hänsch, and J. Reichel, *Nature (London)* **413**, 498 (2001).
- [3] F.L. Moore, J.C. Robinson, C.F. Bharucha, Bala Sundaram, and M.G. Raizen, *Phys. Rev. Lett.* **75**, 4598 (1995).
- [4] G. Casati, B.V. Chirikov, F.M. Izraelev, and J. Ford, in *Lecture Notes in Physics* (Springer-Verlag, Berlin, 1979), Vol. 93, p. 334.
- [5] S. Fishman, D.R. Grempel, and R.E. Prange, *Phys. Rev. Lett.* **49**, 509 (1982).
- [6] E. Ott, in *Chaos in Dynamical Systems* (Cambridge University Press, Cambridge, U.K., 1993); F. Haake, *Quantum Signatures of Chaos* (Springer-Verlag, Berlin, 1991).
- [7] D.A. Steck *et al.*, *Science* **293**, 274 (2001); W.K. Hensiger *et al.*, *Nature (London)* **412**, 52 (2001).
- [8] B.G. Klappauf, W.H. Oskay, D.A. Steck, and M.G. Raizen, *Phys. Rev. Lett.* **81**, 1203 (1998).
- [9] M.B. d'Arcy, R.M. Godun, M. Oberthaler, D. Cassetari, and G.S. Summy, *Phys. Rev. Lett.* **87**, 074102 (2001).
- [10] T. Cheon, P. Exner, and P. Seba, *J. Phys. Soc. Jpn.* **72**, 1087 (2003).
- [11] A.J. Lichtenberg and M.A. Lieberman, *Regular and Chaotic Dynamics* (Springer-Verlag, New York, 1992).
- [12] D.L. Shepelyansky *Phys. Rev. Lett.* **56**, 677 (1986).
- [13] B.G. Klappauf, W.H. Oskay, D.A. Steck, and M.G. Raizen, *Phys. Rev. Lett.* **81**, 4044 (1998).
- [14] T.S. Monteiro, P.A. Dando, N.A.C. Hutchins, and M.R. Isherwood, *Phys. Rev. Lett.* **89**, 194102 (2002).
- [15] P.H. Jones *et al.*, quant-ph/0309149.